Deuteron-deuteron elastic and three- and four-body breakup scattering using the Faddeev-Yakubovskii equations

John F. Carew[*]

Department of Nuclear Science and Technology, Brookhaven National Laboratory, Upton, New York 11973-5000, USA

The deuteron-deuteron elastic and three- and four-body breakup scattering cross section have been calculated using the Faddeev-Yakubovskii (FY) chain-of-partition momentum-space equations. In this calculation the initial two-cluster potential is split into separable and nonseparable components, and the effective potential is reduced to elastic two-body and three- and four-body breakup open channels and a closed-channel many-body contribution. The closed-channel contribution is determined by minimizing a variational bound. The Coulomb interaction was included by expanding the initial and final Coulomb states in a Coulomb-Sturmian basis. The three sets of chain-of-partition integral equations were solved for the elastic and three- and four-body breakup scattering amplitudes. The calculations were performed for the $S = 2$ spin/$L = 0$ angular-momentum state. The elastic and double-breakup calculations were performed for energies up to $E = 5.48$ MeV, while the single-breakup calculations were performed for energies up to $E = 4.17$ MeV. In the case of elastic scattering, the calculated scattering length of $^5a_{dd} = 7.8 \pm 0.3$ fm is in good agreement with a FY cluster reduction calculation. The calculated phase shift is smaller than that predicted by the resonating group model and this difference is believed to be due to the differences in the potential and calculation methods. The breakup cross sections were calculated as a function of initial deuteron momentum and fragmented-deuteron momentum. The $d + d \rightarrow d + n + p$ cross sections were compared with neutron yield measurements and, while the measurements also included the $L > 0$ components, the general features were consistent. Estimates of the calculational uncertainties/bias are provided.

I. INTRODUCTION

Over the past decade there has been a considerable effort in the development and application of the four-body scattering equations. This has included calculations using the Alt-Grassberger-Sandhas (AGS) equations [1] solved in momentum-space [2–5] using the Coulomb screening/renormalization method [6]. Using a single-scattering approximation, these equations have been extended to higher energies and used in analyzing recent three-body (160 MeV) deuteron-deuteron breakup experiments [7]. Several configuration-space approaches have also been used: (a) the hyperspherical-harmonics Kohn variational method used to solve the Schrödinger equation [8,9] and (b) the direct numerical solution method [10–12] and the cluster reduction method [13] used to solve the Faddeev-Yakubovskii equations [14]. In addition, the resonating group model (RGM) has been used to solve the Schrödinger equation using the Kohn-Hulthèn variational principle and perform four-body bound-state and elastic and transfer scattering calculations [15]. These efforts have been focused primarily on the four-body elastic and rearrangement collisions.

A momentum-space variational-bound formulation of the *N*-particle scattering problem has been developed in Ref. [16]. This approach is based on the Faddeev-Yakubovskii chain-of-partition formulation of the *N*-particle equations, and makes use of the chain-space description developed by Benoist-Gueutal and L'Huillier [17] and Cattapan and Vanzani [18]. It is shown that the scattering amplitude for the elastic, rearrangement, and breakup processes satisfies a Lippmann-Schwinger type integral equation in which the kernel integration is over the open channels and the closed channels enter through the effective potential. The effective potential is a scattering operator momentum-space matrix-element consisting of (1) a Born-exchange term of the two-cluster potential between different open-channel states and (2) a term involving the closed channel Green's function. A variational estimate for this second term is obtained when the closed channel Green's functions are estimated using variational upper and/or lower bounds. In this approach the interparticle potential is not assumed to be separable as in typical quasiparticle schemes.

In this paper, the *N*-particle variational-bound equations are applied to the case of deuteron-deuteron elastic, three-body $d + d \rightarrow d + n + p$ breakup and four-body $d + d \rightarrow n + p + n + p$ breakup scattering. The purpose of this effort was to (1) assess the feasibility of four-body elastic and breakup scattering calculations using the momentum-space *N*-particle Faddeev-Yakubovskii equations, (2) solve the set of coupled chain-of-partition transition amplitude integral equations, and (3) identify solution techniques and difficulties (numerical, modeling, etc.) in their application. While the elastic scattering is a simpler and more transparent four-body

---
[*]carew@bnl.gov

calculation, the breakup reactions are considered to be of special importance. Because of their continuum of multiple free-particle final states, it is expected the resulting phase-space will be used in evaluating the scattering dynamics, Coulomb effects and $3N$ force models used in multiparticle calculations.

In Sec. II, the application of the Ref. [16] N-particle methods to the four-body deuteron-deuteron scattering system is described. This includes (a) the separable expansion of the two-cluster open-channel resolvent operator, (b) the description of the open and closed channel contributions to the effective potential, and (c) the coupled elastic and breakup scattering amplitude equations. The calculation methods and results are presented in Sec. III including (a) the scattering length and elastic cross sections with comparisons to alternate methods calculations and (b) the three- and four-body breakup cross sections as a function of the initial relative deuteron momentum and the fragmented-deuteron momentum. A summary of the calculations is presented in Sec. IV and an analysis of the calculational uncertainty and bias is provided in the Appendix.

II. FOUR-BODY INTEGRAL EQUATIONS

A. N-particle chain-labeled pairwise potentials

The N-particle system interacting via pairwise potentials may be described by the Hamiltonian

$$H = H_0 + \sum_{i<j} V_{ij} = H_0 + V, \qquad (1)$$

where H_0 is the center-of-mass free particle energy and V_{ij} is the interaction between particles i and j. Following the Faddeev-Yakubovskii approach, one introduces the partition a_p ($1 \leqslant p \leqslant N$) as a particular decomposition of the N-particle system into a unique grouping of p disjoint (non-interacting) subsets or clusters. A partition b_r that can be formed by decomposing the specific clusters of the partition a_p is considered to follow from partition a_p and satisfies the equation $b_r \subset a_p$. A chain A_p^r of partitions corresponding to the sequential breakup of partition a_p into r-cluster partition a_r is represented as

$$A_p^r = \{a_r \subset a_{r-1}, \ldots, a_{p+1} \subset a_p\}, \quad 1 \leqslant p < r \leqslant N. \quad (2)$$

The chains that are initiated from single cluster partition a_1, A_1^r, and the chains that terminate with N-cluster partition a_N are denoted $A_1^r = A^r$ and $A_r^N = A_r$. The complete chain A is initiated from a_1 and terminated with a_N.

The interaction V_{a_p} internal to partition a_p is the sum of all two-body potentials that are internal to the p clusters of a_p,

$$V_{a_p} = \sum_{a_{N-1} \subset a_p} V_{a_{N-1}}, \qquad (3)$$

where $V_{a_{N-1}}$ is the two-body interaction associated with partition a_{N-1}.

In the case of the deuteron-deuteron scattering system, 18 chains are required to define the chain space. Accounting for particle identity, there are only seven physically distinguishable chains. In this case, there is only one physi-

cally distinguishable chain describing the complete decomposition which is taken to be A_1^4: $(1, 2, \hat{3}, \hat{4}) \rightarrow (1, \hat{4})(2, \hat{3}) \rightarrow (1)(\hat{4})(2, \hat{3}) \rightarrow (1)(2)(\hat{3})(\hat{4})$, where particles 3 and 4 are protons. The three corresponding two-cluster chains are obtained by particle exchange. While these four chains define the initial and final states, all chains/partitions contribute to the total scattering interaction.

B. Separable expansion of the two-cluster open-channel resolvent operator

The effective potential can be determined by separating the energetically allowed open P channels, and noting that the scattering operator associated with a potential $V = V^P + V^Q$ can be written as $T^P + T^Q$ [16]. The closed-channel operator T^Q satisfies the Lippman Schwinger equation

$$T^Q = V^Q + V^Q G_0 T^Q, \qquad (4)$$

where G_0 is the resolvent operator for the unperturbed system. In the case that the potential V supports a set of bound states with state vectors $|\varphi_i\rangle$ and energies ϵ_i, the separable potential is taken to be

$$V^P = \sum_{i,j} V|\varphi_i\rangle (V^{-1})_{ij} \langle \varphi_j|V, \qquad (5)$$

where the matrix V is defined

$$V_{ij} = \langle \varphi_i|V|\varphi_j\rangle. \qquad (6)$$

It then follows from the relation

$$V^Q|\varphi_i\rangle = (V - V^P)|\varphi_i\rangle = 0 \qquad (7)$$

that V^P supports the same $|\varphi_i\rangle$ states. Since V^P is separable, T^P can be determined algebraically and is given by Eq. (10) of Ref. [19]. In the present application, $|\varphi_i\rangle$ are the two-cluster eigenstates of the Hamiltonian H_{a_2} representing the open-channel configurations. Recalling that $G_{a_2} = G_0 + G_0 T_{a_2} G_0$ and taking

$$H_{a_2}^Q = H_0 + V_{a_2}^Q, \qquad (8)$$

it follows that

$$T_{a_2}^Q = V_{a_2}^Q + V_{a_2}^Q G_0 T_{a_2}^Q \qquad (9)$$

and

$$G_{a_2} = G_{a_2}^Q + G_0 T_{a_2}^P G_0. \qquad (10)$$

Using the separable expansion for T^P [19], $G_{a_2}^P$ may be expressed as a sum over open channels: e.g., for the

$d + d \rightarrow d + n + p$ single breakup[1,2]

$$G_{a_2}^P = G_0 T_{a_2}^P G_0 = \int d\mathbf{q}_{a_2} \left|\varphi_{a_2}^D(E - \mathbf{q}_{a_2}^2); \mathbf{q}_{a_2}\right\rangle \frac{\mathbf{S}_{a_2}(E - \mathbf{q}_{a_2}^2)}{E - \mathbf{q}_{a_2}^2 + \epsilon_{a_2}} \left\langle \varphi_{a_2}^{D(-)}(E - \mathbf{q}_{a_2}^2); \mathbf{q}_{a_2}\right|$$

$$+ \sum_{e_3 \subset a_2} \int d\mathbf{q}_{a_2} d\mathbf{p}_{e_3} \left|\varphi_{a_2(e_3)}^D(E - \mathbf{q}_{a_2}^2); \mathbf{q}_{a_2}, \mathbf{p}_{e_3}\right\rangle \frac{\mathbf{S}_{a_2(e_3)}(E - \mathbf{q}_{a_2}^2; \mathbf{p}_{e_3})}{E - \mathbf{q}_{a_2}^2 - \mathbf{p}_{e_3}^2 + \epsilon_{e_3}} \left\langle \varphi_{a_2(e_3)}^{D(-)}(E - \mathbf{q}_{a_2}^2); \mathbf{q}_{a_2}, \mathbf{p}_{e_3}\right|, \tag{11}$$

where the "self-energy" matrices are defined

$$\mathbf{S}_{a_2}^{-1}(E - \mathbf{q}_{a_2}^2) = \left\langle \varphi_{a_2} | \varphi_{a_2}^D(E) \right\rangle \tag{12}$$

and

$$\mathbf{S}_{a_2(e_3)}^{-1}(E - \mathbf{q}_{a_2}^2; \mathbf{p}_{e_3}) = \left\langle \varphi_{a_2(e_3)}^{(-)}(\mathbf{p}_{e_3}) | \varphi_{a_2(e_3)}^D(E; \mathbf{p}_{e_3}) \right\rangle. \tag{13}$$

The distorted bound-state and breakup states are, respectively,

$$\left|\varphi_{a_2}^D(E)\right\rangle = G_{a_2}^Q(E) V_{a_2} |\varphi_{a_2}\rangle \tag{14}$$

and

$$\left|\varphi_{a_2(e_3)}^D(E); \mathbf{p}_{e_3}\right\rangle = G_{a_2}^Q(E) V_{a_2} |\varphi_{a_2(e_3)}(\mathbf{p}_{e_3})\rangle, \tag{15}$$

where $G_{a_2}^Q$ is the resolvent operator associated with the potential $V_{a_2}^Q$ and $\mathbf{p}_{e_3}$ is the relative momentum of the two clusters resulting from the fragmentation. (It is noteworthy that there is no distortion when the states are on shell; i.e., $|\varphi_{a_2}^D\rangle \rightarrow |\varphi_{a_2}\rangle$ when $E = -\epsilon_{a_2}$). The state $|\varphi_{a_2}; \mathbf{q}_{a_2}\rangle$ represents the situation in which the two clusters of partition a_2 move freely with a (renormalized) relative momentum of $\mathbf{q}_{a_2}$, with $|\varphi_{a_2}\rangle$ describing the bound states of the two clusters of partition a_2 with total energy $= -\epsilon_{a_2}$. Similarly, $|\varphi_{a_2(e_3)}; \mathbf{q}_{a_2}, \mathbf{p}_{e_3}\rangle$ represents a scattering state of H_{a_2} in which the initial partition is e_3 ($\subset a_2$) with the two clusters of a_2 having relative momentum $\mathbf{q}_{a_2}$ and the two clusters which are bound in partition a_2 and are fragmented in partition e_3 have relative momentum $\mathbf{p}_{e_3}$. The state $|\varphi_{e_3}\rangle$ describes the initial bound states of the three clusters of partition e_3 with total energy $-\epsilon_{e_3}$. The distorted states $|\varphi_{a_2}^D(E - \mathbf{q}_{a_2}^2); \mathbf{q}_{a_2}\rangle$ and $|\varphi_{a_2(e_3)}^D(E - \mathbf{q}_{a_2}^2); \mathbf{q}_{a_2}, \mathbf{p}_{e_3}\rangle$ in Eq. (11) are obtained by replacing the bound states by the distorted bound states defined in Eqs. (14) and (15).

While the $V_{a_2}^Q$ nonseparable component of the potential is neglected in typical separable expansions, the nonseparable component is included in the present approach. It enters the effective potential calculation through the closed-channel resolvent operator $G_{a_2}^Q$, via the distortion of the initial and final states and as a contribution to the effective potential. In the case of the deuteron-deuteron system, the closed-channel Q-space resolvent operator $G_{a_2}^Q$ is determined by a variational bound procedure.

---

[1]In the case of double breakup, the separable term for the $|\varphi_{a_2(e_4)}^D(E - \mathbf{q}_{a_2}^2); \mathbf{q}_{a_2}, \mathbf{p}_{e_3}, \mathbf{p}_{e_4}\rangle$ four-body breakup state is added to the right-hand side of Eq. (11) when $E > 0$.

[2]For convenience, the energy continuation is suppressed when it is $E + i\epsilon$.

C. Transition amplitudes and the effective potential

In the case of deuteron-deuteron scattering, the Ref. [16] [Eq. (58)] expression for the T_{ij} scattering amplitudes reduces to the following three chains of coupled integral equations: the $d + d \rightarrow d + d$ elastic amplitude

$$T_{11} = V_{11} + T_{11} P_1 V_{11}, \tag{16}$$

the $d + d \rightarrow d + n + p$ breakup amplitudes

$$T_{22} = V_{22} + T_{22} P_2 V_{22}, \tag{17}$$

$$T_{21} = V_{21} + T_{22} P_2 V_{21} + T_{21} P_1 V_{11}, \tag{18}$$

and the $d + d \rightarrow n + p + n + p$ double-breakup amplitudes[3]

$$T_{32} = V_{32} + T_{32} P_2 V_{22}, \tag{19}$$

$$T_{31} = V_{31} + T_{32} P_2 V_{21} + T_{31} P_1 V_{11}. \tag{20}$$

On the left, index 1 corresponds to the final one-momentum symmetrized two-partition $(2,\hat{4})(1,\hat{3})$ free-particle state, index 2 corresponds to the two-momentum symmetrized three-partition $(1)(\hat{3})(2,\hat{4})$ free-particle state, and index 3 corresponds to the three-momentum symmetrized four-partition $(1)(2)(\hat{3})(\hat{4})$ free-particle state. On the right, index 1 corresponds to the initial one-momentum symmetrized two-partition $(1,\hat{4})(2,\hat{3})$ free-particle state and index 2 corresponds to the two-momentum symmetrized three-partition $(2,\hat{3})(1)(\hat{4})$ free-particle state. The propagators $P_1(\mathbf{q}_{a_2}; E)$ and $P_2(\mathbf{q}_{a_2}, \mathbf{p}_{e_3}; E)$ are defined in terms of the self-energy matrices S_i, the cluster-cluster momenta $\mathbf{q}_{a_2}$ and $\mathbf{p}_{e_3}$, and the deuteron cluster binding energy ϵ,

$$P_1(\mathbf{q}_{a_2}; E) = \frac{S_{a_2}(E - \mathbf{q}_{a_2}^2)}{E - \mathbf{q}_{a_2}^2 + 2\epsilon} \tag{21}$$

and

$$P_2(\mathbf{q}_{a_2}, \mathbf{p}_{e_3}; E) = \frac{S_{a_2(e_3)}(E - \mathbf{q}_{a_2}^2; \mathbf{p}_{e_3})}{E - \mathbf{q}_{a_2}^2 - \mathbf{p}_{e_3}^2 + \epsilon}. \tag{22}$$

The deuteron breakup has been included by adding a second separable term to the two-cluster potential, with a deuteron scattering state of momentum $\mathbf{p}_{e_3}$ replacing the bound state. P_1 is the bound-state propagator and P_2 is the corresponding breakup propagator. The distortion of the states

---

[3]In the double-breakup calculations, each fragmented deuteron was assumed to have the same internal momentum and, as a result of momentum constraints, V_{33} and T_{33} are zero.

$|\varphi_{a_2}^D(E - \mathbf{q}_{a_2}^2); \mathbf{q}_{a_2}\rangle$ and $|\varphi_{a_2(e_3)}^D(E - \mathbf{q}_{a_2}^2); \mathbf{q}_{a_2}, \mathbf{p}_{e_3}\rangle$ is caused by the nonseparable component of the potential. These distorted states only appear as final states in the effective potential since there is no distortion of the initial on-shell states.

The effective potential V_{ij} consists of the two terms

$$V_{ij} = B_{ij} + V_{ij}^Q, \tag{23}$$

where the P-space open-channel (cluster-to-cluster) Born-exchange contribution is

$$B_{ij} = \langle \varphi_i^{D\,(-)}|V(2, \hat{4}) + V(1, \hat{3})|\varphi_j\rangle \tag{24}$$

and V_{ij}^Q is the Q-space closed-channel variational contribution. For convenience, in this calculation the $G_{a_2}^Q$ input for the closed-channel variational contribution has been simplified by (1) assuming a single term symmetric trial function g_0 and (2) neglecting the small second-order contributions from the weakend nonseparable potential.[4] The closed-channel variational contribution is then[5]

$$V_{ij}^Q = \frac{4\pi}{D_0} V_i^{(F)} P^Q V_j^{(I)}, \tag{25}$$

where the initial and final chain-dependent potentials are

$$V^{(I)}(1, 1) = \langle g_0|V(1, \hat{4})|\varphi_1\rangle, \tag{26}$$

$$V^{(I)}(1, 2) = \langle g_0|V(2, \hat{3})|\varphi_1\rangle, \tag{27}$$

$$V^{(I)}(2, 1) = \langle g_0|V(1, \hat{4})|\varphi_2\rangle, \tag{28}$$

$$V^{(I)}(2, 2) = \langle g_0|V(2, \hat{3})|\varphi_2\rangle, \tag{29}$$

and $V^{(F)}(i, 1) = V^{(F)}(i, 2) = \langle \varphi_i^{D\,(-)}|V(2, \hat{4}) + V(1, \hat{3})|g_0\rangle.$
$$\tag{30}$$

The Q-space chain-dependent propagators are $P^Q(1, 1) = (1 + a^2)/d$, $P^Q(1, 2) = -a\,(1 + a)/d$, $P^Q(2, 2) = P^Q(1, 1)$, and $P^Q(2, 1) = P^Q(1, 2)$, where $a = \langle g_0|V(1, \hat{4})|g_0\rangle/4D_0$, $d = 1 + a^2 - 2a^3$, and $D_0 = \langle g_0|E - H_0|g_0\rangle$.

The V_{ij}^Q contribution is determined using a variational-bound procedure [16] for determining $G_{a_2}^Q$. Since the weakend closed-channel two-cluster potential $V_{a_2}^Q$ does not support bound states below the four-body threshold (i.e., $E < 2\epsilon = 4.38\,\text{MeV}$), the g_0 trial function is spatially damped and the error in the $G_{a_2}^Q$ estimate can be shown to be of definite sign allowing both upper and lower bound estimates to be determined. In this calculation, the g_0 trial function is determined

by minimizing the variational expression for which the error is known to be positive, providing an upper bound. This g_0 minimization procedure was carried out at each energy $E < 2\epsilon$, providing an energy dependent trial function. When $E > 2\epsilon$, the trial function must include a four-cluster continuum scattering function.[6] Since in these calculations $E \lesssim 2\epsilon$ and V_{ij}^Q is generally small compared to B_{ij}, the energy dependence above $E > 2\epsilon$ was approximated and $V_{ij}^Q(E > 2\epsilon)$ was taken to be $V_{ij}^Q(E = 2\epsilon)$.

In order to account for the Coulomb interaction, the initial and final Coulomb states were each expanded in a Coulomb-Sturmian (CS) basis. This allowed the CS components of these states to be determined analytically. In the case of elastic scattering the expansion was made in terms of the deuteron-deuteron separation, while in the breakup calculations the expansion was made using the proton-proton separation. The calculation of the effective potential matrix elements with respect to the CS basis was reduced to a one-dimensional integration, which was performed numerically. In defining the basis states, the scaling factor of the CS functions was taken to be $3.0\,\text{fm}^{-1}$ consistent with the range of the potential. As in Ref. [20], a smoothing factor was employed to minimize the effect of the Gibbs oscillations as the number of CS expansion terms (NCS) increases. The calculations were performed with a converged CS expansion of NCS = 21 terms.

To minimize calculation uncertainty, numerical techniques including extended-precision coding to eliminate round-off and increase accuracy, range-dependent mesh to improve accuracy, and convergence acceleration to improve efficiency have been employed. As an additional qualification, a detailed and systematic assessment of the calculational uncertainties has been performed. This has included the evaluation of the uncertainties and bias, their propagation through the calculation and their effect on the $d + d$ scattering length and elastic amplitude calculation. This assessment is included in the Appendix.

III. CALCULATION METHODS AND RESULTS

A. Calculation methods

The transition amplitudes were calculated using the set of ten (when the imaginary amplitudes are included) coupled momentum-space integral equations (16)–(20). In solving the coupled equations, the T_{22} and T_{32} intermediate-state amplitudes were determined first, and then substituted into the equations for the T_{21} and T_{31} final-state amplitudes. The real and imaginary amplitude components were uncoupled iteratively.

The calculations were performed for the $S = 2$ spin/$L = 0$ angular momentum state using the Gaussian two-body potential and associated deuteron ($\epsilon = -2.193\,\text{MeV}$) bound-state wave function of Ref. [21].[7] The V_{ij}^Q effective potential was

---

[4]This simplification neglects the nonseparable potential contributions to $G_{a_2}^Q$ [$p = 2$ terms of A in Eq. (62) of [16]].

[5]For convenience, chains 2 and 5 of [16] have been relabeled 1 and 2, respectively.

[6]It is also noteworthy that when $E > 2\epsilon$, the error in the variational estimate is not of definite sign and the usual $G_{a_2}^Q$ bound feature is no longer available.

[7]The Gaussian potential is used here since (1) it allows the effective potential (9D) integrations to be performed analytically and
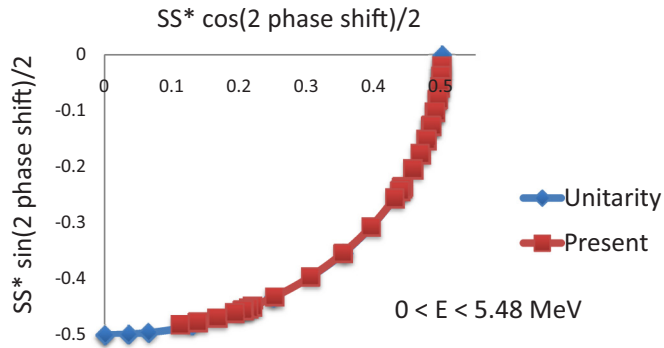
FIG. 1. Elastic unitarity vs phase shift ($-1.1°$ to $-38.5°$) to energies above the four-body breakup threshold for the $S = 2/L = 0$ state. The three- (four-)body threshold is at $-13.7°$ ($31.7°$) to the horizontal.

calculated using an input Green's function determined using the upper-bound variational principle together with the g_0 Gaussian trial function. The $L = 0$ component of the potential was determined by an additional angular integration which was also performed analytically.

As an initial assessment of the calculation methods, the elastic unitarity was calculated for energies up to 5.48 MeV (i.e., above the four-body breakup threshold). The unitarity dependence on phase shift was determined and the calculated SS^* and the $SS^* = 1$ unitarity circle are compared in Fig. 1. Below the three-body breakup threshold (phase shift $= -13.7°$) unitarity is satisfied exactly and the two curves agree to within $\pm 0.01\%$. This agreement is consistent with the accuracy of the T_{11} amplitudes, which was independently determined to be $\pm 0.01\%$. Above the three-body threshold the T_{21} amplitude also contributes to the unitarity sum, which results in a reduction in the T_{11} fractional contribution and a reduction in the radius of the elastic unitarity curve (i.e., SS^* moves toward the inside of the circle). Similarly, above the four-body threshold (phase shift $= -31.7°$) the T_{31} amplitude results in a further reduction in the radius of the elastic unitarity curve. However, because of the reduced magnitude of the breakup cross sections this contribution is very small and the two curves are almost identical. This was confirmed by the elastic channel calculation of $S_{12}^* S_{21} = 1 - S_{11}^* S_{11} = 0.0006$ and the breakup channel calculation, using the T_{21} amplitude, of $S_{12}^* S_{21} = 0.0007$ (the difference being round-off). The breakup calculation involved the summation over both the final state two-body momentum and the fragmented deuteron internal momentum.

At the two breakup thresholds, the SS^* calculations were performed with an extra fine energy mesh to allow a detailed description of the elastic and breakup cross sections and possible threshold anomalies. The calculations, however, indicated no anomalies or significant deviations from the unitarity cir-
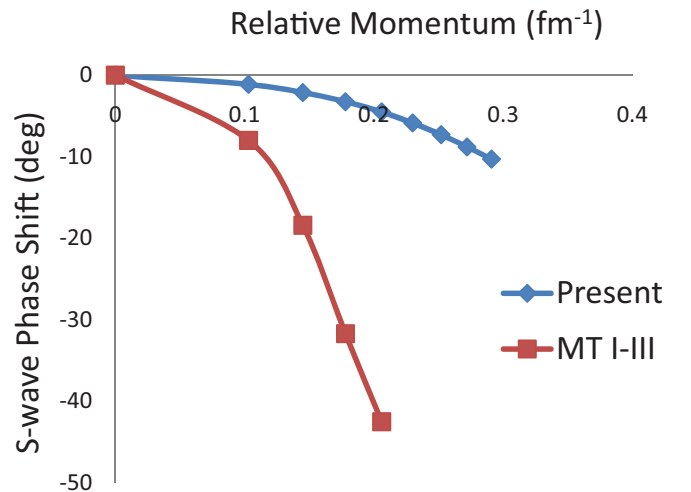
FIG. 2. Deuteron-deuteron $S = 2/L = 0$ scattering phase shift vs the relative momentum, below the three-body breakup threshold ($\kappa = 0.325 \, \mathrm{fm}^{-1}$).

cle. This is believed to be due to the Coulomb repulsion which maintains a large deuteron-deuteron separation at low energy (i.e., just above the threshold). As a result of this barrier the breakup cross section is insensitive to the energy (the cross section and its derivatives tend to zero at the threshold [22]) and no anomaly or cusp is introduced.

B. Elastic scattering

The scattering length calculation was performed using the zero-energy K-matrix form of the $d + d \rightarrow d + d$ elastic chain equation. The elastic $S = 2$ Coulomb-modified scattering length calculation predicted a value of $^5a_{dd} = +7.8 \pm 0.3$ fm.[8] This compares well with the $^5a_{dd} = +7.5$ fm value of Filikhin and Yakovlev (FY) of Ref. [23] calculated using the configuration-space cluster reduction method including Coulomb effects.

The calculated $S = 2/L = 0$ deuteron-deuteron phase shift for momentum below the single-breakup threshold ($\kappa < 0.325 \, \mathrm{fm}^{-1}$) is given in Fig. 2. For comparison, the Filikhin and Yakovlev phase shift calculation using the MT I–III two-body potential [24] is also included. It is seen that the FY phase shift is substantially more negative with a stronger momentum dependence than the present calculation. This difference is believed to be due to the difference in potentials. The Pauli repulsion in the symmetric $S = 2$ spin state ensures the particles are well separated, increasing the sensitivity of the phase shift to the long-range properties of the potential. The effective range of the MT I–III Yukawa potential is a factor of ~ 3 larger than the range of the Gaussian potential used in the present calculation. As indicated in the effective-

---

(2) the kernel of the amplitude momentum-space integral equation is analytic, eliminating the difficulties associated with the complex singularities and contour rotation that occur with Yukawa-type potentials.

---

[8]As described in the Appendix, this value is the result of a recent detailed uncertainty analysis that has been performed for the scattering length calculation and is an update of the $^5a_{dd} = 8.2$ fm value of Ref. [16].
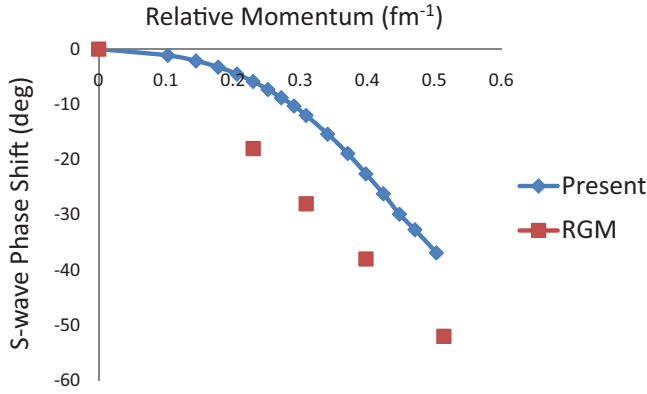
FIG. 3. Deuteron-deuteron $S = 2/L = 0$ scattering phase shift vs the relative momentum, above the four-body breakup threshold ($\kappa = 0.460\,\mathrm{fm}^{-1}$).

range expansion, this will increase the phase shift and result in the observed stronger momentum dependence.[9]

In Fig. 3, the phase shift calculation of Hofmann and Hale (HH) of Ref. [15] is compared with the present calculation. The calculations were performed for momentum above the double-breakup threshold ($\kappa = 0.460\,\mathrm{fm}^{-1}$) up to a momentum of $\kappa = 0.514\,\mathrm{fm}^{-1}$ ($E = 5.48\,\mathrm{MeV}$), and use the RGM with the more recent Bonn-based Gaussian potential of Kellermann *et al.* [26]. While both calculations have the same linear dependence on momentum, the present calculation indicates a smaller phase shift. However, the Bonn-based potential used in the RGM calculation differs in that it includes (1) a strong attractive core for $r \lesssim 1.0\,\mathrm{fm}$ and (2) a slightly weaker attractive long-range tail for $r \gtrsim 1.0\,\mathrm{fm}$. The larger phase shift of the RGM calculation is believed to be due to the strong attractive core of the Bonn-based potential and the difference in the calculation methods.[10] Variational-bound calculations using the Ref. [26] Gaussian Bonn-based potential are presently underway.

C. Three-body $d + d \rightarrow d + n + p$ breakup scattering

The breakup cross section was calculated for the cases where the fragmented deuteron takes the specific fragmented-deuteron kinetic energy fractions FKE = 0.1, 0.5, and 0.9 of the available ($\kappa > 0.325\,\mathrm{fm}^{-1}$) initial kinetic energy. The calculations were performed as a function of initial relative deuteron momentum up to a value of $\kappa = 0.449\,\mathrm{fm}^{-1}$ ($E = 4.17\,\mathrm{MeV}$). The $S = 2/L = 0$ Coulomb-

---

[9]While the FY and present predictions of the phase shift disagree, the zero-energy scattering length predictions are in good agreement. This insensitivity of the scattering length to the potential is consistent with previous 4N calculations in which the particles are well separated [25].

[10]The Ref. [26] potential consists of (17) damped Gaussian terms and the effective range is similar to that of the Gaussian used in the present calculation. Consequently, unlike the difference with the FY calculation, this difference in phase shift cannot be explained by a difference in the effective range of the potentials.
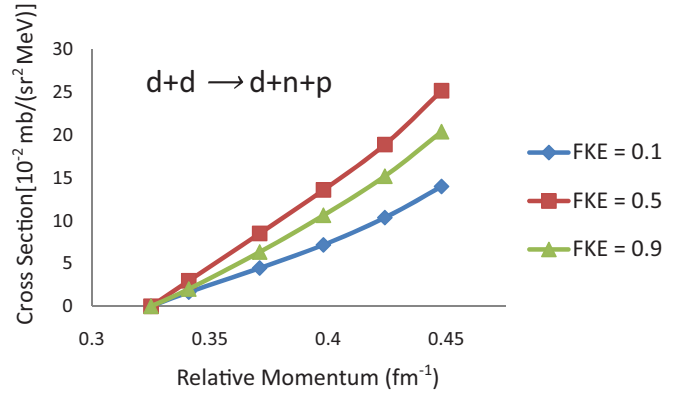

FIG. 4. $d + d \rightarrow d + n + p$ $S = 2/L = 0$ breakup cross section vs the initial deuteron relative momentum, as a function of the fragmented-deuteron kinetic energy fraction (FKE).

corrected breakup cross section for these cases is given in Fig. 4 as a function of the initial relative deuteron momentum.

The breakup cross section was also calculated as a function of FKE at $E = 3.29\,\mathrm{MeV}$ ($\kappa = 0.398\,\mathrm{fm}^{-1}$). The normalized breakup cross section and Coulomb-corrected cross section are presented in Fig. 5. For comparison, the normalized $D(d,np)D$ neutron yield measured by Cranberg *et al.* [27] at $E = 3.15\,\mathrm{MeV}$ and zero degrees (with the beam) is also presented. Comparing the measured neutron yield and the uncorrected breakup cross section, it is seen that both the measured and calculated peaks occur at FKE ~ 0.40. However, the measurement is significantly more peaked than the calculation. The effective potential includes terms that contribute exponential factors of the form $\exp(\alpha\kappa \cdot \mathbf{K})$, where $\mathbf{K}$ is the deuteron-deuteron relative momentum, which would produce the stronger peak. However, these terms do not contribute in the $L = 0$ calculation. On the other hand, the measurements of Cranberg and those of Cabral *et al.* [28] include a strong angular dependence indicating the presence of the $L > 0$ contributions which would explain the sharper peak in the measurements.
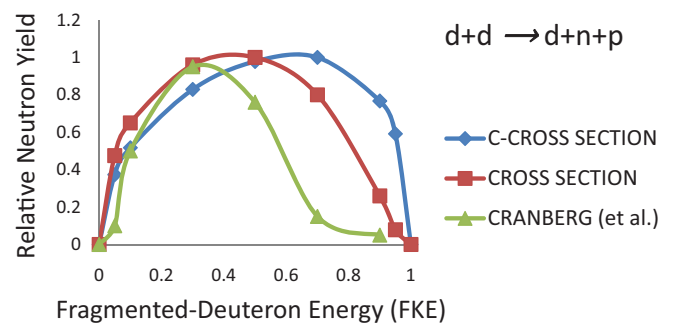

FIG. 5. Relative neutron yield for the $d + d \rightarrow d + n + p$ reaction vs the fragmented-deuteron kinetic energy fraction (FKE), together with the (normalized) cross sections and Coulomb-corrected cross sections. Calculations are at 3.29 MeV and the Cranberg *et al.* measurements are at 3.15 MeV.
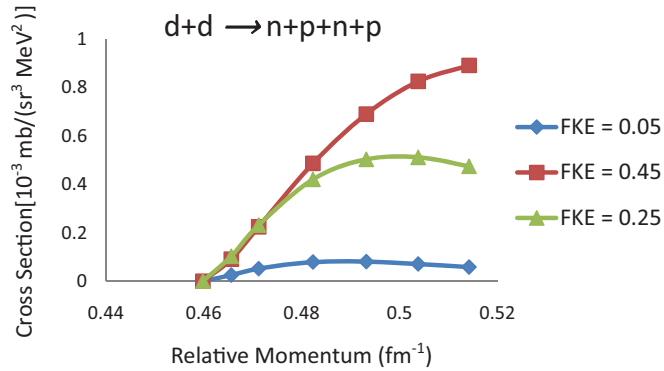
FIG. 6. $d + d \rightarrow n + p + n + p$ $S = 2/L = 0$ breakup cross section vs the initial deuteron relative momentum, as a function of the fragmented-deuteron kinetic energy fraction (FKE).

D. Four-body $d + d \rightarrow n + p + n + p$ breakup scattering

The breakup cross section was calculated for the cases where the fragmented deuterons each take an equal fraction FKE = 0.05, 0.25, and 0.45 of the available ($\kappa >$ 0.460 fm^{-1}) initial kinetic energy. The calculations were performed as a function of the initial relative deuteron momentum up to a value of $\kappa = 0.514$ fm^{-1} ($E = 5.48$ MeV). The $S = 2/L = 0$ Coulomb-corrected breakup cross section for these cases is given in Fig. 6 as a function of the initial relative deuteron momentum.

The breakup cross section was also calculated as a function of FKE at $E = 4.82$ MeV ($\kappa = 0.482$ fm^{-1}). The normalized breakup cross section and Coulomb-corrected breakup cross section are presented in Fig. 7. The breakup cross section peaks at FKE ~ 0.25. The Coulomb correction is especially large at FKE ~ 0.45, where the fragmented-deuteron energy is large and the proton-proton energy is low. This reduces the proton penetration factor C_0 and decreases the Coulomb uncorrected cross section in Fig. 7. This is exacerbated by the fact that the available energy in this case is only 0.434 MeV compared to the three-body breakup where the available energy is 1.097 MeV.

IV. SUMMARY

The deuteron-deuteron elastic, three-body, and four-body breakup scattering cross sections have been calculated using the Faddeev-Yakubovskii chain-of-partition momentum-space equations as described in Ref. [16]. In this approach the initial two-cluster potential is split into separable and non-separable components, and the scattering amplitudes satisfy a Lippmann-Schwinger type equation in which the kernel integration is over the open channels and the closed channels enter through the effective potential. The effective potential consists of a P-space open-channel Born-exchange term and a Q-space closed-channel variational contribution. The effective potential closed-channel term is determined by minimizing a variational bound. The Coulomb effects are included by expanding the initial and final Coulomb states in a Coulomb-Sturmian basis.

The three sets of chain-of-partition momentum-space integral equations were solved for the elastic and three- and four-body breakup scattering amplitudes. The calculations were performed for the $S = 2$ spin/$L = 0$ angular-momentum state. In the case of elastic scattering, the calculated scattering length of $^5a_{dd} = 7.8 \pm 0.3$ fm compares well with the $^5a_{dd} = +7.5$ fm value of Ref. [23] calculated using the configuration-space cluster reduction method. However, the calculated phase shift is smaller than that predicted by the RGM calculation of Ref. [15]. This difference is believed to be due to the different potentials and methods used in the calculations.

The $d + d \rightarrow d + n + p$ breakup cross sections were calculated as a function of initial deuteron momentum and fragmented-deuteron energy. The cross sections were compared with neutron yield measurements and, while the measurements also included the $L > 0$ angular-momentum and spin < 2 components, the general features were consistent. The $d + d \rightarrow n + p + n + p$ breakup cross sections were also calculated as a function of initial deuteron momentum and fragmented-deuteron energy. No comparisons were made for the double breakup since applicable measurements were not available. Estimates of the calculational uncertainties and bias were also provided.

APPENDIX: UNCERTAINTY ANALYSIS FOR THE DEUTERON-DEUTERON SCATTERING CALCULATIONS

1. Scattering length calculation

The variational-bound formulation of the N-particle scattering problem based on the Faddeev-Yakubovskii equations is given in Ref. [16]. This integral-equation formulation, implemented using a set of specially designed numerical methods, has been applied to the two-cluster case of deuteron-deuteron scattering. Using this approach, the $S = 2$ deuteron-deuteron scattering length is calculated to be $^5a_{dd} = +8.2$ fm.

The various many-body techniques developed for the $N \geqslant 4$ particle systems necessarily include a number of difficult to assess approximations. In order to assess the effect of the calculational uncertainties introduced by the approximations and numerical methods used in the scattering length
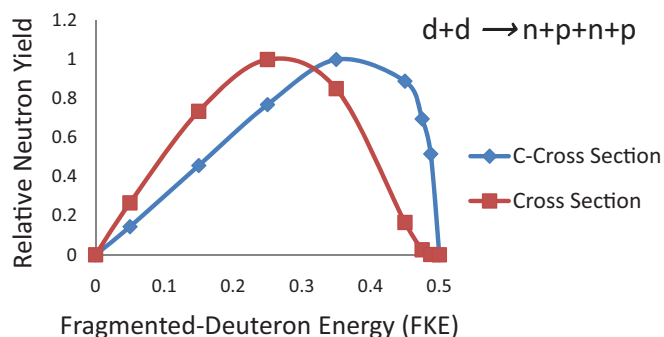

FIG. 7. Normalized cross sections and Coulomb-corrected cross sections (i.e., the relative neutron yield) for the $d + d \rightarrow n + p + n + p$ reaction vs the fragmented-deuteron kinetic energy fraction (FKE) at 4.82 MeV.

TABLE I. Effect of approximations and numerical methods uncertainties and bias on the deuteron-deuteron scattering length calculation.

Source of bias/uncertainty	Bias (fm)	Uncertainty (fm)
Born-exchange term spatial integration	0.0	±0.09
Variational-bound trial function	+0.1	±0.01
Second-order Born distortion	0.0	±0.2
Distortion coarse-mesh momentum	−1.3	±0.1
Coulomb-Sturmian convergence	+0.8	±0.1
Integration and summation of CS terms	0.0	±0.1
Smoothing numerics	0.0	±0.06
Total	−0.4	±0.3
$^5a_{dd} = 8.2 +$ bias $\pm$ uncertainty $= 7.8 \pm 0.3$ fm		

calculation a detailed uncertainty analysis has been performed. This analysis included (a) the identification of the significant sources of systematic bias and random uncertainties, (b) the estimation of these biases and (1σ) uncertainties, and (c) the determination of their effects on the deuteron-deuteron scattering length calculation.

The results of this analysis are summarized in Table I. The determination of the B_{ij} Born-exchange term in the effective potential [Eq. (24)] requires a two-dimensional spatial integration. This integration was performed numerically using two methods: (1) as a two-dimensional integral and (2) as the product of two one-dimensional integrals in a series expansion. A comparison of these two methods indicated a scattering length uncertainty of ±0.09 fm with no systematic bias.[11] The closed-channel Q-space contribution to the effective potential [Eq. (25)] was determined using the upper-bound variational principle for the Q-space Green's function. The selection of the trial function in this variational calculation also introduces uncertainty. Based on sensitivity studies of the upper bound, it is estimated this term contributes a scattering length bias of +0.1 fm and an uncertainty of ±0.1 fm.

The determination of the off-shell long-range distortion of the deuteron bound states [Eqs. (14) and (15)], by the nonseparable component of the potential V^Q, requires the solution of a (negative-energy) Lippmann-Schwinger type integral equation for $G^Q_{a_2}(E)$. Since the potential V^Q is weak and to avoid the large momentum-space matrix inversion, $G^Q_{a_2}(E)$ was approximated with $G_0(E)$. To evaluate this approximation, the second-order Born contribution was added. Comparing these calculations, it was determined that the $G_0(E)$ calculation of the distorted bound states introduces a scattering length uncertainty of ±0.2 fm and no bias. In addition, to reduce

computing time a relatively coarse mesh was used to represent the distortion momentum dependence. A fine mesh calculation indicated a scattering length bias of −1.3 fm and an uncertainty of ±0.1 fm.

To minimize numerical uncertainty in the determination of the Coulomb-Sturmian components of the initial and final states, an accurate integration of the individual terms of the CS expansion and their summation is required. This calculation has been performed using both a numerical and analytic approach. Comparison of the results of these calculations indicates a scattering length uncertainty of ±0.1 fm and no systematic bias. Based on the observed asymptotic dependence of the scattering length on the number of CS expansion terms, it is estimated the numerics of the smoothing process used to minimize the effect of Gibbs oscillations contribute a ±0.06 fm uncertainty. No bias is indicated.

In order to assess the accuracy of the Coulomb-Sturmian representation of the initial and final states, the order of the expansion was increased to tighten the convergence (NCS = 25terms). The results indicated a scattering length bias of +0.8 fm and an uncertainty of ±0.1 fm.

Applying these statistical bias/uncertainty data, the base calculation is updated in Table I leading to a deuteron-deuteron scattering length of $^5a_{dd} = +7.8 \pm 0.3$ fm. This variational (momentum-space) integral-equation calculation is in good agreement with the cluster-reduction (configuration-space) integrodifferential equation result of $^5a_{dd} = +7.5$ fm [23].

2. Scattering amplitude calculations

The zero-energy K-matrix scattering length and the $E > 0$ elastic T-matrix amplitude calculations differ in that the T-matrix calculation includes a pole in the two-body momentum integration. The methods for treating this pole are well established and introduce no significant additional uncertainty/bias. The calculation of the effective potential is the same in both cases. The self-energy matrices, bound-state distortion, and propagators are determined using the exact same methods in these calculations. The numerical solution of the K-matrix and T-matrix integral equations has been verified and is not a significant contributor to the uncertainty. The Coulomb-Sturmian expansion is the same. As a result it is expected the elastic amplitude calculational uncertainty will be similar to that of the scattering length calculation.

In the case of the $E > \epsilon$ breakup amplitude calculations, the inhomogeneous terms of the integral equations [Eqs. (18) and (20)] include the T_{22} and T_{32} amplitudes and the uncertainty and bias observed in the scattering length are not applicable. In addition, the $E > 2\epsilon$ four-body breakup effective potential does not include the required four-cluster continuum scattering trial function. It is expected the use of the approximate energy-independent $V^Q_{ij}(E = 2\epsilon)$ potential above $E > 2\epsilon$ will increase the uncertainty/bias as energy increases. The uncertainty analysis for the breakup amplitudes will be performed after the inclusion of the free-particle scattering term in the $E > 2\epsilon$ trial function.

---

[11]It should be noted that the bias and uncertainty values given here are applicable for the specific parameters and methods used in this calculation. It is expected these uncertainties/biases can be reduced by further tightening of the methods.

[1] P. Grassberger and W. Sandhas, Nucl. Phys. B. **2**, 181 (1967); E. O. Alt, P. Grassberger, and W. Sandhas, JINR Report No. E4-6688, 1972 (unpublished).

[2] A. Deltuva and A. C. Fonseca, Phys. Rev. C **75**, 014005 (2007).

[3] A. Deltuva and A. C. Fonseca, Phys. Rev. Lett. **98**, 162502 (2007).

[4] A. Deltuva and A. C. Fonseca, Phys. Rev. C **87**, 054002 (2013).

[5] A. Deltuva and A. C. Fonseca, Phys. Rev. C **92**, 024001 (2015).

[6] A. Deltuva, A. C. Fonseca, and P. U. Sauer, Annu. Rev. Nucl. Part. Sci. **58**, 27 (2008).

[7] I. Ciepał, K. Bodek, N. Kalantar-Nayestanaki, G. Khatri, St. Kistryn, B. Kłos, A. Kozela, J. Kuboś, P. Kulessa, A. Łobejko, A. Magiera, I. Mazumdar, J. Messchendorp, W. Parol, D. Rozpędzik, I. Skwira-Chalot, E. Stephan, A. Wilczek, B. Włoch, A. Wrońska, and J. Zejma, Few-Body Syst. **60**, 44 (2019).

[8] M. Viviani, A. Kievsky, S. Rosati, E. A. George, and L. D. Knutson, Phys. Rev. Lett. **86**, 3739 (2001).

[9] A. Kievsky, S. Rosati, M. Viviani, L. E. Marcucci, and L. Girlanda, J. Phys. G **35**, 063101 (2008).

[10] R. Lazauskas and J. Carbonell, Phys. Rev. C **70**, 044002 (2004).

[11] R. Lazauskas, Phys. Rev. C **79**, 054007 (2009).

[12] K. Hebeler, H. Krebs, E. Epelbaum, J. Golak, and R. Skibinski, Phys. Rev. C **91**, 044001(R) (2015).

[13] I. N. Filikhin and S. L. Yakovlev, Phys. At. Nucl. **63**, 55 (2000).

[14] O. A. Yakubovskii, Sov. J. Nucl. Phys. **5**, 937 (1967).

[15] H. M. Hofmann and G. M. Hale, Phys. Rev. C **77**, 044002 (2008).

[16] J. F. Carew, Few-Body Syst. **55**, 171 (2014).

[17] P. Benoist-Gueutal and M. L'Huillier, J. Math. Phys. (NY) **23**, 1823 (1982).

[18] G. Cattapan and V. Vanzani, Nuovo Cimento **A89**, 29 (1985).

[19] J. Carew and L. Rosenberg, Phys. Rev. C **5**, 658 (1972).

[20] Z. Papp, Phys. Rev. C **55**, 1080 (1997).

[21] R. S. Christian and J. L. Gammel, Phys. Rev. **91**, 100 (1953).

[22] R. G. Newton, in *Scattering Theory of Waves and Particles* (McGraw-Hill, New York, 1966), p. 541.

[23] I. N. Filikhin and S. L. Yakovlev, Phys. At. Nucl. **63**, 216 (2000).

[24] R. A. Malfliet and J. A. Tjon, Ann. Phys. (NY) **61**, 425 (1970).

[25] S. K. Adhikari and K. L. Kowalski, in *Dynamical Collision Theory and its Applications* (Academic, San Diego, 1991), p. 382.

[26] H. Kellermann, H. M. Hofmann, and C. Elster, Few-Body Syst. **7**, 31 (1989).

[27] L. Cranberg, A. H. Armstrong, and R. L. Henkel, Phys. Rev. **104**, 1639 (1956).

[28] S. Cabral, G. Börker, H. Klein, and W. Mannhart, Nucl. Sci. Eng. **106**, 308 (1990).